

# Transfer Film Tenacity: A Case Study Using Ultra-Low-Wear Alumina–PTFE

J. Ye<sup>1,3</sup> · A. C. Moore<sup>2</sup> · D. L. Burris<sup>1,2</sup>

Received: 9 June 2015 / Accepted: 3 August 2015 / Published online: 15 August 2015  
© Springer Science+Business Media New York 2015

**Abstract** The transfer film, a protective barrier that forms when a solid lubricant slides against a hard and high-surface-energy counterface, plays an important role in friction and wear reduction. The transfer films of many solid lubricants are removed and replenished during sliding. However, one particularly low wear rate solid lubricant has been shown to produce persistent transfer films that thicken and homogenize over the course of a test. Based on a mass balance of the system, transfer film growth can only occur if its wear rate is less than that of the parent polymer. However, recent measurements of the wear rates of these transfer films show that they are likely orders of magnitude higher than those of the parent polymer. The goal of this paper is to elucidate the origins of this apparent contradiction. In this study, a high-density polyethylene (HDPE) probe was used in an effort to approximate the contact conditions under which the film originally formed. Transfer films formed during run-in of the parent solid lubricant were removed immediately by the HDPE pin ( $k \sim 10^0 \text{ mm}^3/\text{Nm}$ ). However, transfer films formed after the solid lubricant had transitioned to ultra-low wear rates themselves exhibited ultra-low wear rates in the range from  $10^{-8}$  to  $10^{-10} \text{ mm}^3/\text{Nm}$ ; to our knowledge, this is the first direct observation of ultra-low wear rate transfer films, a condition that was previously assumed necessary for ultra-low wear rates of the

solid lubricant system. Follow-up measurements showed that the wear rate of the transfer film was extremely sensitive to the surface energy of the probe; the wear rate increased by orders of magnitude when the surface energy of the probe exceeded a critical value near  $\sim 35 \text{ mJ}/\text{mm}^2$ . These results provide fresh insights into the wear behaviors of transfer films and the processes governing ultra-low wear of solid lubricant materials.

**Keywords** Polymer tribology · Transfer film · Wear · Adhesion · Surface energy

## 1 Introduction

Solid lubricant polymers generally have lower moduli and surface energies than opposing counterface materials, which are often ferrous. As the contact moves, adherent debris is left behind to form what is known as the transfer film [1, 2]. The transfer film protects the parent polymer from the counterface on subsequent contacts and therefore reduces the wear rate of the polymer. Fillers that successfully reduce friction and wear of polymers also produce thinner and more uniform transfer films [3–6]. As a result, the wear-reducing action of fillers in polymers is often attributed to the fillers' ability to improve transfer film thickness, uniformity, or adhesion [7].

Naturally, the ability of the transfer film to protect the polymer is limited by its ability to adhere to the counterface. Briscoe [1], who was among the earliest investigators of this problem, found that the best fillers degrade the polymer; he proposed that fillers reduce polymer wear by improving the bond between the transfer film and the counterface. Schwartz and Bahadur [8] showed that the peel strength of a copper tab glued to a PPS nanocomposite transfer film

✉ D. L. Burris  
dlburris@udel.edu

<sup>1</sup> Department of Mechanical Engineering, University of Delaware, Newark, DE 19716, USA

<sup>2</sup> Department of Biomedical Engineering, University of Delaware, Newark, DE 19716, USA

<sup>3</sup> Present Address: Institute of Tribology, Hefei University of Technology, Hefei, Anhui, China

increased with the wear resistance of the nanocomposite. Wang and Yan [9] slid a steel ball against pre-developed polytetrafluoroethylene (PTFE) composite transfer films and showed that the composite transfer films were more wear resistant than the unfilled PTFE transfer films. Li et al. [10] showed that the wear rate of copper-filled PTFE transfer films depended strongly on the film morphology and the conditions under which the film was deposited.

Bahadur and Tabor [4] drew a different conclusion about the role of the filler. They found that pre-deposited composite transfer films had no wear-reducing effect on unreinforced PTFE. Furthermore, even the best PTFE-based composite transfer films were easily removed and immediately replenished by the next pass of the pin. They concluded that improved transfer films of PTFE-based materials must be consequences of small wear debris and not themselves the cause of low wear.

More recently, however, several PTFE-based systems have demonstrated transfer films with significant residence time during dry sliding [9–12]. Ye et al. [12] used optical microscopy to observe the evolution of the transfer films of a particularly wear-resistant PTFE-based material. As with most PTFE composites, debris was removed and replenished each cycle during run-in. However, at a transition point the counterface became populated with nanoscale debris fragments that were persistent and appeared to nucleate the transfer film. These nucleated transfer films thickened and homogenized for the remainder of the test, which indicates that the wear rate of the transfer film must have been lower than that of the ultra-low wear rate polymer pin [5]. Recent studies by Pitenis et al. [13] and Harris et al. [14] elucidated the tribochemical mechanism that is likely responsible for the strong adhesion observed experimentally.

Urueña et al. [11] used microtribometry to directly measure the wear rate of this particular transfer film. They interrupted the wear test after various sliding distances in order to test the wear resistance of the transfer film during run-in and after the transition to ultra-low wear. They found that the wear rate of the transfer film decreased as the wear rate of the polymer pin decreased. However, despite the strong correlation between the transfer film and pin wear rates, the wear rate of the transfer film exceeded that of the pin by orders of magnitude at steady state; the transfer film could not grow if this were the case in situ [12].

The goal of this paper is to elucidate the discrepancy between the ultra-low wear rates of transfer films observed indirectly as they form and the more moderate values obtained when measured directly. During the parent pin-on-flat experiment, the transfer film is exposed to a relatively low-surface-energy material ( $\gamma \sim 20 \text{ mJ/mm}^2$ ) with a relatively low contact pressure ( $\sim 6 \text{ MPa}$ ). We propose that previous wear rate measurements of this transfer film

were artificially elevated due to excessive contact pressure, surface energy, or a combination thereof. In this paper, we use a high-density polyethylene (HDPE) probe to study the wear rate of these transfer films in contact conditions that approximate those in which they were formed.

## 2 Methods

### 2.1 Materials

The composite material used in this study was identical to those reported in our previous studies [12, 15] and comparable to those reported by other groups [13, 16–21]. The matrix material, Teflon<sup>TM</sup> 7C molding resin from DuPont, had a reported particle diameter of  $40 \mu\text{m}$ . The filler material, alpha-phase aluminum oxide ( $\alpha\text{-Al}_2\text{O}_3$ ) nanoparticles from Nanostructured & Amorphous Materials Inc, had a reported particle diameter of  $27\text{--}43 \text{ nm}$ . The filler and matrix powders were combined at 5 wt% loading and hand-shaken to achieve gross homogeneity. Two parts by volume anhydrous ethanol was added to one part of the powder ensemble prior to dispersion by a 500 W ultrasonic horn; power was applied for two of every three seconds over five total minutes. The bulk of the ethanol was drained through laboratory filter paper, and the powder ensemble was dried fully under rough vacuum at  $100 \text{ }^\circ\text{C}$ . The dried powder was loaded into a mold and cold pressed using 100 MPa of pressure into a green sample with a diameter of  $12.5 \text{ mm}$  and a length of  $25 \text{ mm}$ . The green sample was sintered by ramping to  $365 \text{ }^\circ\text{C}$  over 3 h, sitting at  $365 \text{ }^\circ\text{C}$  for 3 h, and then cooling uniformly over 3 h.

### 2.2 Transfer Film Preparation

The sintered nanocomposite specimen was machined into a  $6.4 \times 6.4 \times 12 \text{ mm}$  pin. The counterface was made from 304 stainless steel ( $38 \times 25.4 \times 4 \text{ mm}$ ) and polished to a roughness of  $R_a = 20 \text{ nm}$ . Tests were performed at  $25 \text{ }^\circ\text{C}$  in laboratory air on a pin-on-flat linear reciprocating tribometer previously reported [12]. The sliding conditions were identical to those of comparable studies [6, 13, 18, 19, 21, 22] of this tribological pair with a normal load of 250 N, contact pressure of 6.5 MPa, reciprocating length of 25.4 mm, and sliding speed of 50.8 mm/s. The wear test was interrupted periodically for mass loss measurements of the pin with a Mettler Toledo mass balance ( $\pm 10 \mu\text{g}$ ); tests were interrupted at 0.4, 0.8, 2, 3.5, 9.3, 27, 66, 259, 1016, and 4572 m, to capture run-in, transition, and steady-state transfer films, which have been shown to be fundamentally different [12, 15]. Instantaneous wear rates were calculated using a linear regression of the data adjacent to the point of interest using a method reported previously [12].

### 2.3 Characterizing Transfer Film Wear Rate

The custom in situ linear reciprocating tribometer illustrated in Fig. 1 was used to characterize wear rates of the transfer films. Friction and normal forces were measured with a six-channel ATI Nano-17 load cell. An HDPE sphere of 3.175 mm radius was chosen as the pin; HDPE is many orders of magnitude more wear resistant than PTFE, but has similar surface energy and Young's modulus. Prior to each test, the pin was cleaned with ethanol and a lint-free wipe. The normal load was 1 N, the measured contact radius was between 200 and 250  $\mu\text{m}$ , and the mean contact pressure was 5–8 MPa; this is comparable to the contact pressure of the parent test in which the transfer films were created. The sliding speed was limited to 10 mm/s, and the reciprocating length (one direction) was 1.5 mm.

In situ optical microscopy measurements were made before the pin touched the surface and after  $N$  cycles of sliding as shown in Fig. 2a, b. Custom image processing software was used to measure the worn area. The 0 cycle and  $N$  cycle images (a comparison pair) were first aligned and then subtracted to obtain a map of intensity differences (Fig. 2c). A threshold halfway between the intensities representative of the film and counterface was chosen to detect whether wear occurred at any given location. This method was repeated three times for each compared pair to obtain the mean volume lost.

Tests were stopped on the first interruption for which the worn area exceeded 50 % the wear track (Fig. 2d). In the case of very wear resistant films, the HDPE probe eventually liberated one or more debris particles; tests were stopped when transfer from the probe was detected. The initial 0 cycle image and the last image not confounded by probe transfer were used to quantify the total area loss. The mean wear rate of the transfer film was determined using

the mean area loss ( $A_{\text{loss}}$ ), film thickness ( $t$ , based on 10 repeat AFM measurements), normal force ( $F_n$ ), number of cycles ( $N$ ), and stroke ( $s$ ):

$$K_{\text{film}} = \frac{A_{\text{loss}} \cdot t}{F_n \cdot N \cdot 2s} \quad (1)$$

Uncertainties in wear rate measurements were determined using the law of propagation of uncertainty [23–25]. Uncertainties in normal force, number of cycles, and distance per cycle were negligible compared to uncertainties in area loss and film thickness. The standard deviation in thickness over 10 measurements of randomly selected locations was used as the uncertainty in thickness of each film. In cases for which repeat wear tests were performed, area uncertainty is the standard deviation from  $N$  repeat measurements. In cases for which only  $N = 1$  wear test was performed, the area uncertainty was the standard deviation in areas based on three independent images taken of the same wear track; this uncertainty represents the error contribution from the method itself and was typically between 2000 and 2500  $\mu\text{m}$ .

### 2.4 Characterizing Transfer Film Adhesion

The tensile strip test originally proposed by Agrawal and Raj [26] was used to directly measure the ratio of adhesive strength to cohesive strength; we call this the strength ratio,  $\tau^*$ . The method is illustrated in Fig. 3. Transfer films were deposited onto soft-tempered 316 stainless steel sheets of 0.127 mm thickness using otherwise identical conditions to those of the wear tests. The transfer film covered sheets were cut into 2-mm-wide strips along the sliding direction and loaded onto a tensile load frame. The samples were pulled in tension until a regular transverse cracking pattern stabilized within the transfer film. The average crack spacing,  $\lambda$ , was

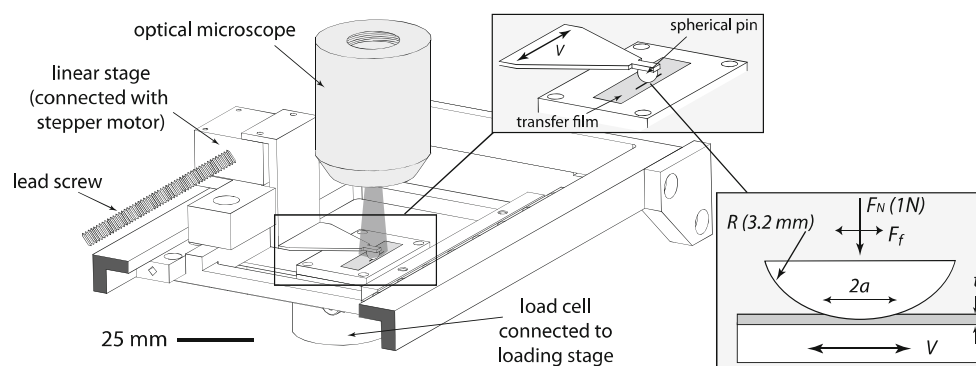


**Fig. 1** Microtribometer used for characterizing the wear rate of the transfer film ( $K_{\text{film}}$ ). A small HDPE spherical pin (radius,  $R = 3.175$  mm) is connected with a linearly reciprocating stage and is loaded (mean pressure of  $P = 6.5$  MPa at a normal force of  $F_n = 1$  N) against the transfer film. The sliding speed is  $V = 10$  mm/s,

and the reciprocating cycle is  $s = 1.5$  mm long. A six-channel load cell fixed beneath the transfer film sample measures the friction and the normal forces. A Nikon<sup>TM</sup> microscope was positioned on top of the wear track to capture the wear of the transfer film optically during sliding

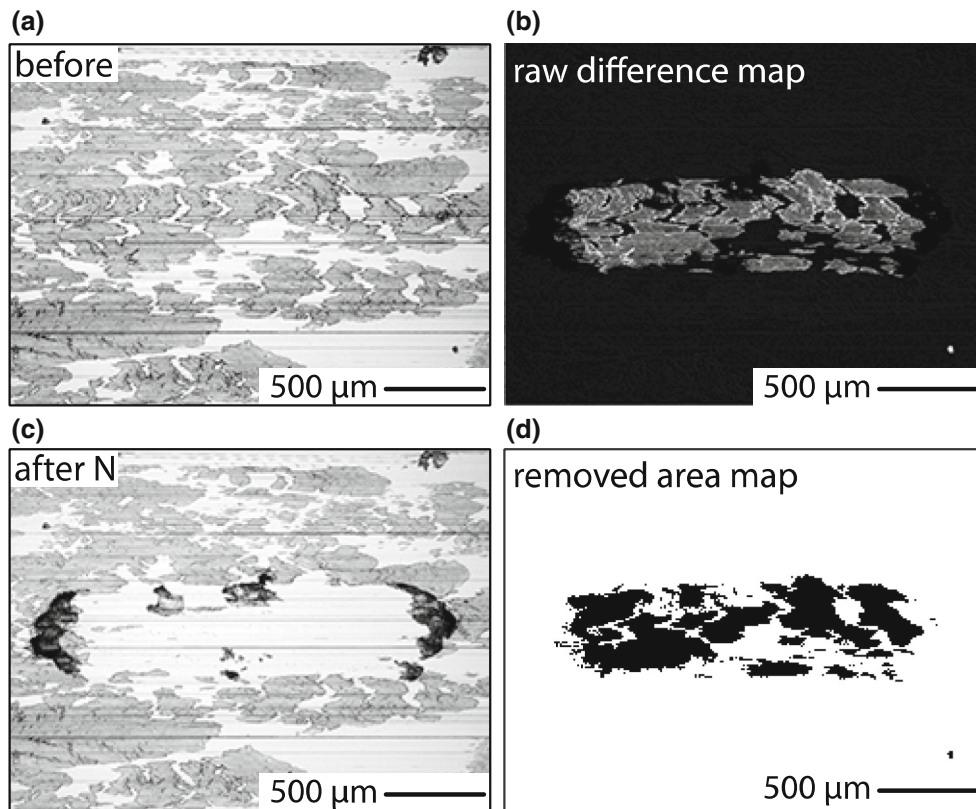


**Fig. 2** Illustration of the method to quantify area loss ( $A_{loss}$ ) of the transfer film. High-resolution images of the transfer film before (a) and after (b) the wear test are first aligned manually using Photoshop™. The corresponding pixel value differences (subtract

(a) from (b)) are calculated and plotted in c where the bright area corresponds to the removed transfer film. A threshold is used to identify areas of removed film (d); these differential areas are added to obtain the total area lost ( $50 \times 10^4 \mu m^2$  in this case)

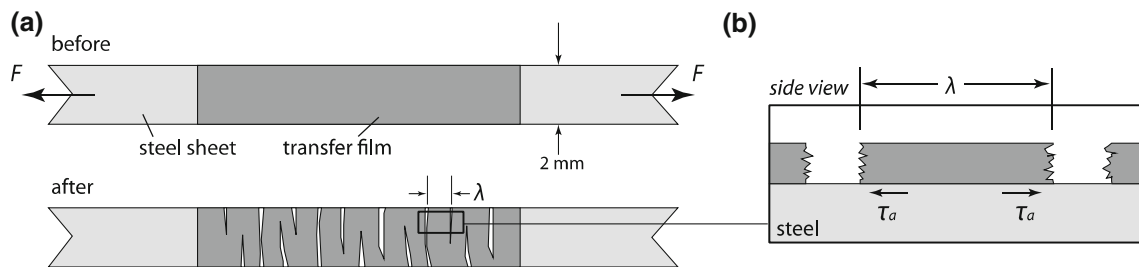


**Fig. 3** A schematic of the tensile strip test used to characterize the transfer film's strength ratio. **a** A sample with a pre-deposited transfer film was pulled in tension along the sliding direction in the native wear tests until transverse cracks within the film initiated. **b** The

transverse cracks induced by the plastic deformation have an average crack spacing of  $\lambda$ . This value was found to be inversely proportional to the adhesion shear strength at the film–substrate interface [26]

measured with a calibrated optical microscope. Agrawal and Raj [26, 27] showed that the average crack spacing ( $\lambda$ ) depends on the ultimate adhesive shear strength ( $\tau_a$ ) and the cohesive tensile strength ( $\sigma_c$ ) of the film:

$$\lambda = \pi \cdot t \cdot \frac{\sigma_c}{\tau_a} \tag{2}$$

To enable comparison between cohesive and adhesive strengths, the Tresca failure criterion [28] is used to rewrite Eq. 2 in terms of shear strengths only,

$$\tau^* = \frac{\tau_c}{\tau_a} = \frac{2 \cdot \pi \cdot t}{\lambda} \tag{3}$$

**Table 1** Properties of the transfer film as a function of the sliding distance and nanocomposite pin wear rate (HDPE probe)

Transfer film samples	Sliding distance to form transfer film (m)	Film thickness ( $\mu\text{m}$ ), $N = 10$	Strength ratio ( $\tau_a/\tau_c$ ), $N$ measurements	Sliding cycles before test stoppage	Wear rate of transfer film, $K_{\text{film}}$ ( $10^{-6} \text{ mm}^3/\text{Nm}$ ), $N$ measurements	Wear rate of polymer pin, $K$ ( $10^{-6} \text{ mm}^3/\text{Nm}$ )
Run-in	0.4	$2.838 \pm 0.779$	$0.18 \pm 0.05$ , 6	1	$340,000 \pm 200,000$ , 5	$260 \pm 53$
	0.8	$1.911 \pm 0.464$	$0.23 \pm 0.07$ , 9	1	$250,000 \pm 120,000$ , 5	$94 \pm 48$
	2.0	$0.901 \pm 0.348$	$0.15 \pm 0.06$ , 4	1	$120,000 \pm 90,000$ , 5	$27 \pm 6$
	3.5	$0.226 \pm 0.056$	$0.32 \pm 0.10$ , 10	1	$33,000 \pm 18,000$ , 5	$13 \pm 6$
Transition	9.3	$0.019 \pm 0.004$	N/A	1000	$0.0171 \pm 0.0185$ , 1	$0.12 \pm 0.06$
	27	$0.045 \pm 0.006$	N/A	10000	$0.0018 \pm 0.0090$ , 1	$0.12 \pm 0.06$
	66	$0.067 \pm 0.025$	N/A	50000	$0.0002 \pm 0.0052$ , 1	$0.10 \pm 0.06$
Steady state	259	$0.077 \pm 0.020$	$1.58 \pm 0.17$ , 6	50000	$0.0008 \pm 0.0006$ , 3	$0.07 \pm 0.04$
	1016	$0.342 \pm 0.044$	$1.64 \pm 0.26$ , 5	100000	$0.0069 \pm 0.0040$ , 2	$0.34 \pm 0.18$
	4572	$0.843 \pm 0.178$	$1.84 \pm 0.18$ , 5	920000	$0.0036 \pm 0.0036$ , 1	$0.12 \pm 0.04$

Each value is reported as the mean  $\pm$  the 95 % confidence interval

### 3 Results

#### 3.1 Macrotribometry Wear Testing and Transfer Film Preparation

The wear rates of the polymer nanocomposite during the creation of the transfer films (shown in Table 1) are consistent with those found for this material system in the literature. During the run-in period (first 5 m), wear rates decreased monotonically with distance in the range from  $k \sim 10^{-4}$  to  $k \sim 10^{-5} \text{ mm}^3/\text{Nm}$ . The transfer film, which was initially several microns thick, thinned monotonically with increased sliding distance and decreased wear rate. The transfer film became persistent and wear rates decreased by  $\sim 100\times$  at a point we define as the transition (9 m); this observation supports the idea that transfer film adhesion is a primary mechanism of wear resistance [1]. During the transition, transfer films consist of nanoscale debris fragments [12]. At 200 m of sliding, these fragments had aggregated to form a continuous transfer film that persisted for the remainder of the experiment. At steady state, wear rates of the polymer pin stay near  $k \sim 10^{-7} \text{ mm}^3/\text{Nm}$ , which is the typically cited value for this material [13, 16–21].

#### 3.2 Transfer Film Wear

Representative images of unworn and worn transfer films are shown for run-in, transition, and steady-state conditions in Fig. 4. Each of the four run-in films was completely removed by the initial pass of the HDPE pin (Fig. 4a). The wear rate in each case ranged from 0.033 to 0.34  $\text{mm}^3/\text{Nm}$  (only different because thickness varies), which is orders of

magnitude higher than the corresponding wear rate of the polymer pin ( $0.13\text{--}2.6 \times 10^{-4} \text{ mm}^3/\text{Nm}$ ). This is consistent with the observation that transfer films are removed and replenished on every cycle in the actual wear test [12]. Following the transition, wear rate measurement uncertainties exceeded the measured wear rate due primarily to uncertainty in area loss (islands approached optical resolution); only subtle evidence of transfer film wear was observed before HDPE transfer became detectable after 10,000 cycles (Fig. 4b). This observation too is consistent with wear tests of the nanocomposite pin; it was at this point that debris fragments first adhered to the counterface and remained adhered for many cycles if not indefinitely [12]. Steady-state transfer films ran an order of magnitude longer without visual evidence of HDPE transfer, possibly due to the fact that films were thicker, more continuous, and more protective against the counterface. In this case, HDPE pin transfer can be seen with the naked eye on the left of the track as highlighted in Fig. 4c.<sup>1</sup> The transition and steady-state transfer films were on the order of  $100\times$  more wear resistant than the ultra-low wear pin itself at steady state.

Wear rate is plotted versus distance of transfer film development for the nanocomposite pin and the resulting transfer film in Fig. 5a. The pin and the transfer film have virtually identical trends throughout the test; wear rates

<sup>1</sup> Based on the wear scar in Fig. 4d, the worn radius is  $\sim 400 \mu\text{m}$ . The volume of this spherical cap would be  $0.006 \text{ mm}^3$ , but most of the contact appears to have been brightened by asperity flattening rather than gross removal. There is evidence of a discrete wear event that reflects the liberated debris we saw on the transfer film before stopping the test; these results suggest that wear occurred primarily in this single event. Based on particle size, we estimate that the HDPE had a net wear rate  $k = 3 \times 10^{-7} \text{ mm}^3/\text{Nm}$ .



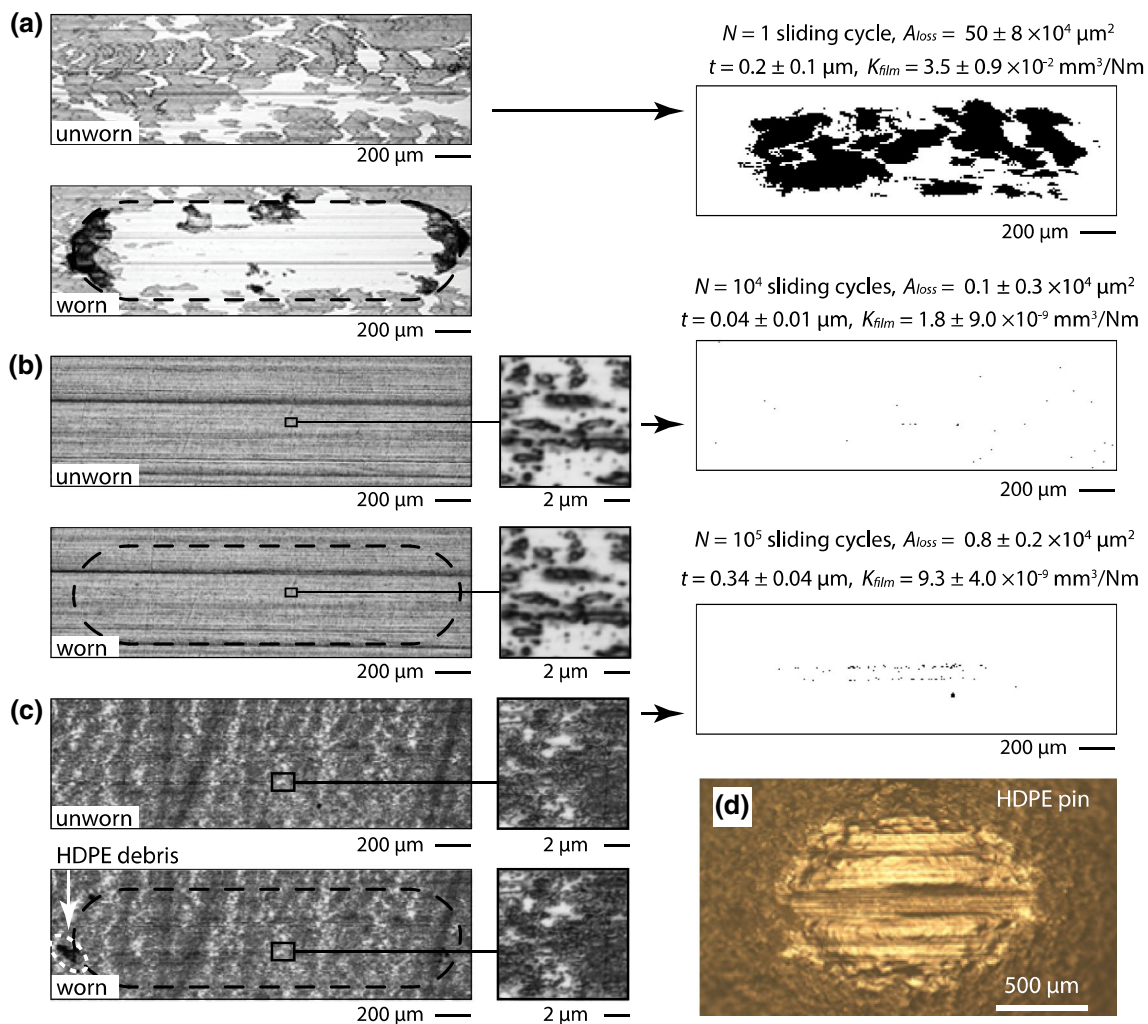


**Fig. 4** Representative transfer film wear rate ( $K_{film}$ ) measurements of the run-in (a), transition (b), and steady-state (c) films. Microtribometry sliding conditions were identical (HDPE probe,  $F_N = 1$  N,  $P = 6.5$  MPa,  $V = 10$  mm/s,  $s = 1.5$  mm) for all tests. The run-in transfer film was removed immediately after the first sliding cycle.

were high initially, decreased during run-in, dropped abruptly at the transition, and eventually crept upward toward a low steady-state value. Interestingly, transfer films always have higher wear rates than the polymer pin before the transition and lower wear rates after the transition. Based on a simple mass balance, transfer films must thin before the transition and thicken after the transition, which is consistent with previous observations [15] and the thickness measurements in this study (Table 1). The wear rate of the nanocomposite pin is plotted against the wear rate of the transfer film in Fig. 5b; the strong correlation supports the hypothesis that the wear resistance of the system is a function of the wear resistance of the transfer film [1].

The transition and steady-state films showed nearly zero wear after prolonged sliding cycles. Transfer film wear resistance improved eight orders of magnitude from the run-in to transition phase of transfer film development

### 3.3 Transfer Film Strength Ratio Measurements

Representative transfer film adhesion/strength ratio measurements of one run-in and one steady-state transfer film are shown in Fig. 6. Both areas of observation have a film thickness of roughly  $1 \mu\text{m}$ . Based on these crack spacing measurements, the steady-state film ( $\lambda = 5 \mu\text{m}$ ) has roughly  $10\times$  the adhesive strength per unit cohesive strength of the run-in film ( $\lambda = 50 \mu\text{m}$ ).

The strength ratio of the transfer film is plotted versus number of development cycles in Fig. 7a. All of the run-in films had shear strength ratios of less than 1, which suggests that delamination is favored over cohesive failure. Conversely, all of the steady-state transfer films had shear strength

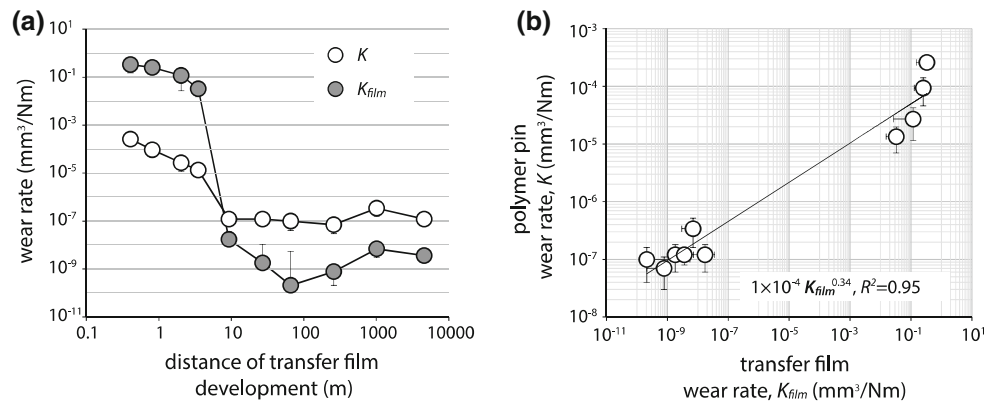


**Fig. 5 a** Wear rates of the polymer pin ( $K$ ) and the transfer film ( $K_{film}$ ) versus distance of transfer film development in macrotribometry experiment. Measurement uncertainty of  $K_{film}$  was calculated based on the uncertainties from image thresholding and film thickness

measurements. All *error bars* represent the 95 % confidence interval. **b** Polymer pin wear rate versus transfer film wear rate. A least squares power law fit is shown for reference

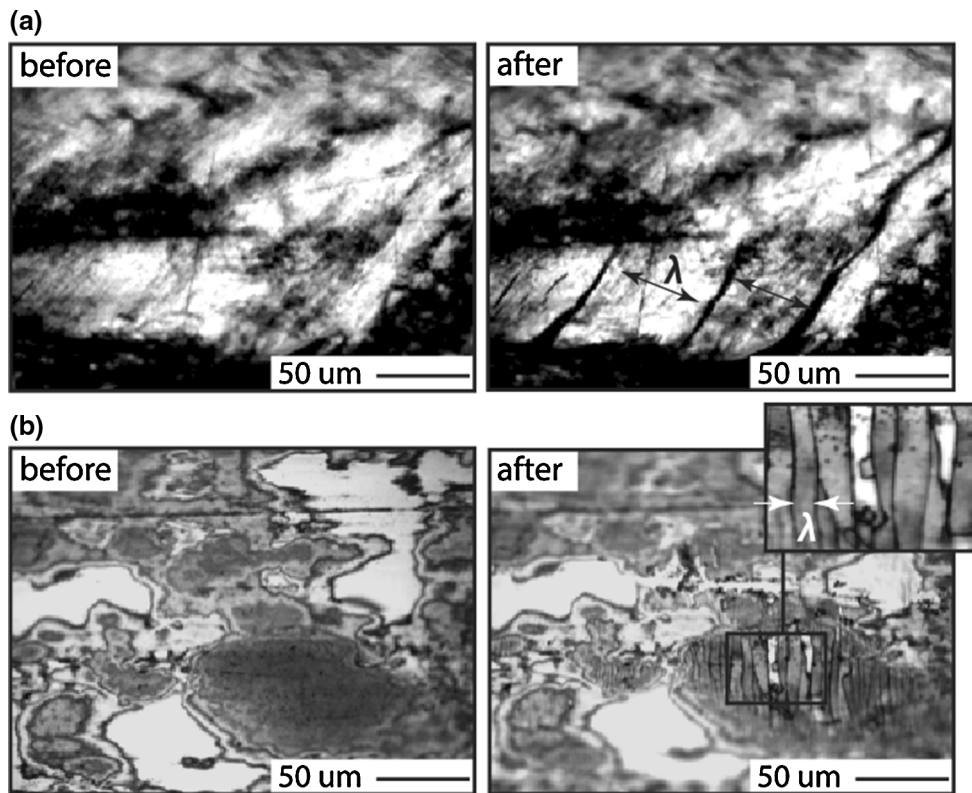


**Fig. 6** Representative strength ratio measurements of a run-in (a) and a steady-state (b) transfer film. Average crack spacing,  $\lambda$ , is measured

optically using Photoshop<sup>TM</sup> and the corresponding strength ratio,  $\tau^*$ , is calculated using Eq. 3

ratios greater than 1, which suggests that cohesive failure is favored over delamination. Transition films were too thin and spatially isolated to produce measurable cracks. The predicted life of the transfer film ranges from 1 to 100 cycles for run-in films with  $\tau^* < 1$  to  $10^8$ – $10^9$  cycles for steady-state films with  $\tau^* > 1$ . The results are consistent with the hypothesis that transfer films are adherent if and only if  $\tau^* > 1$ .

#### 4 Discussion

The primary aim of this paper was to demonstrate that these transfer films are capable of ultra-low wear rates. During transition and steady-state periods in which the native wear tests gave wear rates of  $10^{-7}$  mm<sup>3</sup>/Nm, the wear rates of corresponding transfer films were in the range

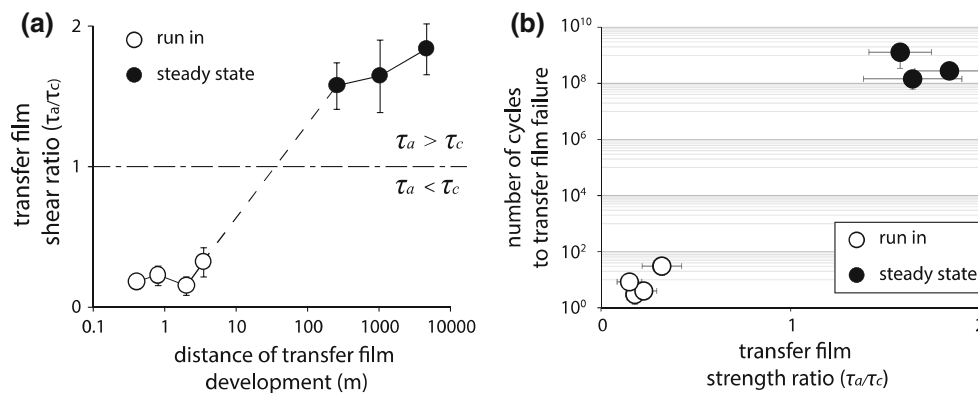


**Fig. 7** **a** Transfer film strength ratio versus macrotribometry sliding distance of transfer film development. Each data point represents 5–10 repeat measurements, and *error bars* represent the 95 % confidence interval. There is a significant increase in transfer film adhesion

strength from the run-in to the steady-state phase of sliding, and all the steady-state films have a higher adhesive than cohesive strength ( $\tau_a/\tau_c > 1$ ). **b** Predicted number of microtribometry sliding cycles until failure versus transfer film strength ratio,  $\tau^*$

**Table 2** Results of steady-state transfer film (developed over 4572 meters of sliding) wear tests when slid against probes of varying material

Probe material	Probe surface energy, $\gamma$ (mJ/m <sup>2</sup> )	Probe modulus (GPa)	Mean contact pressure (MPa)	Mean friction coefficient ( $\mu$ )	Mean shear stress (MPa)	Wear rate of transfer film, $K_{\text{film}}$ ( $10^{-6}$ mm <sup>3</sup> /Nm)
PTFE	18 ± 2	0.5 ± 0.2	6.0 ± 0.2	0.13 ± 0.01	0.77 ± 0.08	0.0050 ± 0.0100
HDPE	30 ± 2	1.0 ± 0.2	19.0 ± 0.3	0.14 ± 0.02	2.64 ± 0.38	0.0036 ± 0.0036
Acetal	36 ± 2	2.9 ± 0.2	47.0 ± 4.7	0.17 ± 0.07	7.90 ± 3.48	2.85 ± 1.20
Acrylic	38 ± 2	3.0 ± 0.2	8.3 ± 0.7	0.54 ± 0.22	4.52 ± 1.85	62.7 ± 26.4
Rubber	41 ± 3	0.05 ± 0.04	0.7 ± 0.1	0.90 ± 0.10	0.63 ± 0.09	350 ± 148
Nylon	46 ± 5	3.0 ± 1.0	8.9 ± 0.7	0.46 ± 0.06	4.04 ± 0.63	110 ± 46
Glass	375 ± 125	70 ± 20	65.3 ± 5.2	0.15 ± 0.10	9.84 ± 6.39	615 ± 259
Steel	900 ± 200	200 ± 20	31.8 ± 4.0	0.11 ± 0.08	3.37 ± 2.54	628 ± 265

The material properties were taken from [29–32]. The contact pressure was calculated using the normal load and the measured contact radius. The friction coefficient was measured directly, and the mean shear stress was calculated as the product of friction coefficient and mean pressure. Measured values are given ± the 95 % confidence interval

from  $10^{-10}$  to  $10^{-8}$  mm<sup>3</sup>/Nm. To the best of our knowledge, this is the first study to report direct measurements of ultra-low wear rates for transfer films.

The wear rates from our study are orders of magnitude lower than those reported previously for nominally identical transfer films [11]. One potentially confounding difference between studies is the roughness of the counterface on which transfer films were deposited; Urueña et al. [11] reports  $R_a \sim 150$  nm, while ours were closer to  $R_a \sim 20$  nm. Additionally, their steel probe had a greater modulus and surface energy than the HDPE probe in this study. To test the relative effects of contact pressure and interfacial adhesion on transfer film wear rates, wear tests of steady-state transfer films were repeated with probes of varying combinations of high versus low modulus and high versus low surface energy. The reported properties of the probes used are provided in Table 2.

Remarkably, the wear rate of the same steady-state film varied by more than 5 orders of magnitude ( $3 \times 10^{-9}$ – $6 \times 10^{-4}$  mm<sup>3</sup>/Nm) when tested against eight probes of varying material properties. Contrary to our expectation, neither contact pressure nor shear stress showed any obvious effect on the wear rate of the transfer film (Table 2). The surface energy of the probe, on the other hand, had a profound effect on the transfer film wear rate as shown in Fig. 8a. The wear rate transitions between very low and very high values near a critical probe surface energy of 35 mJ/m<sup>2</sup>. Interestingly, Blanchet et al. showed similar wear rate toggling for similar PTFE composites when filler loading, particle size, or counterface roughness passed a critical point [16], which suggests that transfer film and system wear rates are driven by the same mechanisms. Figure 8 indicates that the orders of magnitude differences in the wear rates reported here and those from



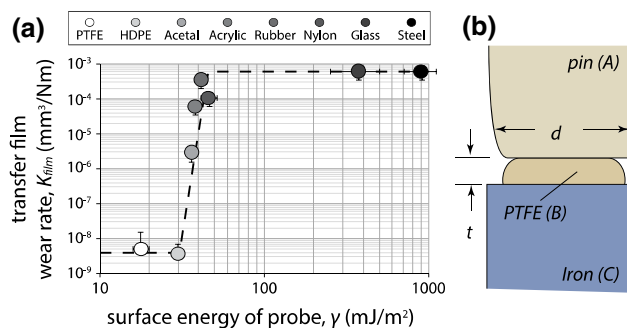


**Fig. 8** **a** Surface energies of the probes versus transfer film wear rates in microtribometry experiments. Error bars represent the 95 % confidence interval. **b** Three-body wear model involving a pin (A), transfer film (B), and counterface (C)

Urueña et al. [11] are due primarily to differences in probe surface energy not contact pressure or surface roughness. The results also indicate that when loaded against a relatively low-surface-energy material like the nanocomposite pin, PTFE, or polyethylene, the transfer film itself provides fantastically low wear rates.

The results remind us that the wear rate is strongly system-dependent and not a material property. Consider the three-body wear situation in Fig. 8b. All three bodies prefer to adhere at two interfaces because adhesive junctions have less energy than free surfaces. The work of adhesion at interface AB, for example, has the form:

$$W_{AB} = c_n(\gamma_A + \gamma_B),$$

where  $\gamma$  is surface energy of each material and  $c_n$  is the compatibility coefficient. Rabinowicz recommends using  $c_n = 1$  for identical non-metals,  $c_n = 0.6$  for compatible non-metals, and  $c_n = 0.36$  for incompatible non-metals [33]; for ease of discussion, we use 0.6 for all non-identical pairs (including PTFE against the PTFE-based nanocomposite). The pins (surface A) and counterface (surface C) have the surface energies listed in Table 2. As previous studies have shown [13, 14, 34, 35], the steady-state transfer films contain significant quantities of  $-\text{COOH}$ , which can increase surface energy of PTFE by up to 30 % [36]. Additionally, the composite contains  $\sim 2.5$  % alumina ( $600 \text{ mJ/m}^2$ ), which, based on a linear rule of mixtures, would further increase surface energy to  $\gamma_B = 38 \text{ mJ/m}^2$ .

The most likely failure interface is the one with the lowest work of adhesion; only the steel probe should be capable of removing the film from the counterface, but our experimental results show high wear rates for probe surface energies as low as  $38 \text{ mJ/m}^2$ . As Gong et al. [37] point out, cohesive failure within the film is also possible; in this case,  $c_n = 1$ ,  $W_{BB} = 76 \text{ mJ/m}^2$  and failure within the film

should be favorable over delamination. Equating  $W_{BB}$  and  $W_{AB} = 0.6 \cdot (\gamma_A + \gamma_B)$  gives a critical probe surface energy for cohesive failure:  $\gamma_{Ac} = 89 \text{ mJ/m}^2$ . Above this value, we expect cohesive failure and high transfer film wear rates. Below this value, we expect adhesive failure at the pin–film interface (AB), interfacial slip at a single interface, and ultra-low wear rates. The experiments bear out such a transition, but at less than half this expected critical value:  $\gamma_A = 30\text{--}40 \text{ mJ/m}^2$  (Fig. 8a). We believe that statistical variation in material properties is responsible for this lower-than-predicted critical value.

The above analysis fails to explain why the HDPE probe was able to easily remove run-in transfer films from the counterface. As Bahadur and Tabor [4] point out, most transfer films of PTFE do not adhere at all but are simply pushed out of the way and subsequently replenished. This system reflects a balance between adhesive energy and elastic energy [33]. The loaded island in Fig. 8b is under a compressive load that is approximately equal to its yield strength ( $S_y$ ). Once the load is removed, adhesion fights the contractile Poisson effect. The island pops free when stored elastic energy exceeds the adhesive energy or when  $t > \frac{2 \cdot W_{BC} \cdot E}{S_y^2 \cdot \nu^2} \sim 3 \text{ }\mu\text{m}$  [33] ( $E$  is Young's modulus and  $\nu$  is Poisson's ratio). The debris must reach a critically small size before they become adherent and much smaller yet before they adhere strongly.

The above analysis suggests several important features of ultra-low wear rate solid lubricants. First, a weak but stable sliding interface between the solid lubricant and counterface is not likely. The low-surface-energy solid lubricant will transfer to the higher-surface-energy counterface to reduce energy; we believe this is the reason the steel probe removes the transfer film so effectively [11]. Second, the transfer film must be stable to prevent intermittent exposure of the high-surface-energy counterface; the higher the surface energy of the counterface, the lower the strength of the solid lubricant, and the smaller the debris, the more adherent the transfer film will be. On this basis, it is logical that decreased wear rates should accompany reduced debris size and improved transfer film coverage, which is observed experimentally [3]. Third, the pin–film interface must be weaker than the film and the pin. In our experiment, we reduce compatibility with dissimilar materials. However, when the PTFE composite lays down its own transfer film, the two surfaces should be perfectly compatible and there should be no single weak interface; yet, we consistently find that the system achieves ultra-low wear rates [6, 16, 17, 19–22]. When solid lubricants lay their own transfer films, it is possible that localized structural or compositional changes near the interface reduce compatibility and weaken the interface. Hu et al. [38], for

example, found significant lamellar ordering of a Mo-W-S-Se composite coatings within 10 nm of the sliding interface, and our recent studies of this PTFE system showed significant compositional differences between the transfer film, the running surface of the polymer pin, and the bulk of the polymer pin [34].

Although the surface energy approach taken here provides some basic insights into the phenomena observed in this study, it is clearly oversimplified. The stability of a weak interface can involve material properties, surface texture, operating conditions (*e.g.*, pressure, speed, and temperature), and even environmental constituents. It has been shown, for example, that roughening [16] or orienting the counterface texture [6] can disrupt low wear. It is also known that environmental humidity can be used to destabilize the weak interface [13, 14, 18, 21, 34, 35, 39, 40]. The development and stability of these weak interfaces are an interesting open question with critical implications for the design of next-generation solid lubricants.

## 5 Conclusion

During run-in when the pin wore at high wear rates, the corresponding transfer film wore at even higher wear rates against an HDPE probe. The films were removed on the first pass, suggesting they do not adhere to a meaningful degree. The adhesive strength of the film was less than its cohesive strength at this point in the test.

During steady state when the pin wore at ultra-low wear rates, the corresponding transfer film wore at even lower wear rates against HDPE. Adhesion measurements revealed that the adhesive strength increased by an order of magnitude compared to that of the run-in film; it exceeded the film's cohesive strength, which suggests that wear is favored over delamination at steady state.

Ultra-low wear occurred for probes with surface energy below a critical value. In such cases, weak but stable interfaces emerged between the pin and the film.

For probes of higher surface energy, the weak interface was located within the film, at the film-counterface interface, or a combination thereof. Varying probe material caused the wear rate of the transfer film to vary by five orders of magnitude.

The results reinforce the fact that the wear rate is not a material property but a system property. Characterization of wear rates for the purpose of predicting life requires careful consideration of the sliding conditions in the application of interest.

**Acknowledgments** The authors gratefully acknowledge financial support from the AFOSR (YIP FA9550-10-1-0295) for financial support of this work.

## References

1. Briscoe, B.: Wear of polymers—an essay on fundamental aspects. *Tribol. Int.* **14**, 231–243 (1981)
2. Lancaster, J.K.: Polymer-based bearing materials—role of fillers and fiber reinforcement. *Tribol. Int.* **5**, 249–255 (1972)
3. Bahadur, S., Gong, D.: The action of fillers in the modification of the tribological behavior of polymers. *Wear* **158**, 41–59 (1992)
4. Bahadur, S., Tabor, D.: The wear of filled polytetrafluoroethylene. *Wear* **98**, 1–13 (1984)
5. Blanchet, T., Kennedy, F.: Sliding wear mechanism of polytetrafluoroethylene (PTFE) and PTFE composites. *Wear* **153**, 229–243 (1992)
6. Burris, D., Sawyer, W.: Tribological sensitivity of PTFE/alumina nanocomposites to a range of traditional surface finishes. *Tribol. T.* **48**, 147–153 (2005)
7. Burris, D.L., et al.: Polymeric nanocomposites for tribological applications. *Macrol. Mater. Eng.* **292**, 387–402 (2007)
8. Schwartz, C., Bahadur, S.: Studies on the tribological behavior and transfer film-counterface bond strength for polyphenylene sulfide filled with nanoscale alumina particles. *Wear* **237**, 261–273 (2000)
9. Wang, Y.X., Yan, F.Y.: Tribological properties of transfer films of PTFE-based composites. *Wear* **261**, 1359–1366 (2006)
10. Li, H., et al.: A study of the tribological behavior of transfer films of PTFE composites formed under different loads, speeds and morphologies of the counterface. *Wear* **328–329**, 17–27 (2015)
11. Uruena, J.M., et al.: Evolution and wear of fluoropolymer transfer films. *Tribol. Lett.* **57**, 1–8 (2015)
12. Ye, J., Khare, H.S., Burris, D.L.: Transfer Film evolution and its role in promoting ultra-low wear of a PTFE nanocomposite. *Wear* **297**, 1095–1102 (2013)
13. Pitenis, A.A., et al.: Ultra-low wear PTFE and alumina composites: all about tribochemistry. *Tribol. Lett.* **57**, 626–631 (2015)
14. Harris, K.L., et al.: PTFE tribology and the role of mechanochemistry in the development of protective surface films. *Macromolecules* **48**, 3739–3745 (2015)
15. Ye, J., Khare, H.S., Burris, D.L.: Quantitative characterization of solid lubricant transfer film quality. *Wear* **316**, 133–143 (2014)
16. Blanchet, T.A., Kandanur, S.S., Schadler, L.S.: Coupled effect of filler content and countersurface roughness on PTFE nanocomposite wear resistance. *Tribol. Lett.* **40**, 11–21 (2010)
17. Kandanur, S.: The role of filler size & content and countersurface roughness in the wear resistance of alumina-PTFE nanocomposites. Ph.D. Rensselaer Polytechnic Institute (2010)
18. Krick, B.A., et al.: Environmental dependence of ultra-low wear behavior of polytetrafluoroethylene (PTFE) and alumina composites suggests tribochemical mechanisms. *Tribol. Int.* **51**, 42–46 (2012)
19. Krick, B.A., Ewin, J.J., McCumiskey, E.J.: Tribofilm formation and run-in behavior in ultra-low-wearing polytetrafluoroethylene (PTFE) and alumina nanocomposites. *Tribol. T.* **57**, 1058–1065 (2014)
20. McElwain, S., et al.: Effect of particle size on the wear resistance of alumina-filled PTFE micro- and nanocomposites. *Tribol. T.* **51**, 247–253 (2008)
21. Pitenis, A.A., et al.: In vacuo tribological behavior of polytetrafluoroethylene (PTFE) and alumina nanocomposites: the importance of water for ultralow wear. *Tribol. Lett.* **53**, 189–197 (2014)
22. Burris, D., Sawyer, W.: Improved wear resistance in alumina-PTFE nanocomposites with irregular shaped nanoparticles. *Wear* **260**, 915–918 (2006)
23. Burris, D.L., Sawyer, W.G.: Measurement uncertainties in wear rates. *Tribol. Lett.* **36**, 81–87 (2009)

24. Schmitz, T., et al.: Wear-rate uncertainty analysis. *J. Tribol.-T. ASME*. **126**, 802–808 (2004)
25. I.S.O. (ISO): Guide to the Expression of Uncertainty in Measurement (Corrected and Reprinted 1995). (1993)
26. Agrawal, D.C., Raj, R.: Measurement of the ultimate shear-strength of a metal ceramic interface. *Acta Metall. Mater.* **37**, 1265–1270 (1989)
27. Agrawal, D.C., Raj, R.: Ultimate shear strengths of copper silica and nickel silica interfaces. *Mat. Sci. Eng. A-Struct.* **126**, 125–131 (1990)
28. Liu, K., Piggott, M.R.: Shear-strength of polymers and fiber composites. 1. Thermoplastic and thermoset polymers. *Composites*. **26**, 829–840 (1995)
29. Brandrup, J., Immergut, E.H. and G. E.A., *Polymer Handbook*. Wiley, New York (1999)
30. Cognard, P., *Handbook of Adhesives and Sealants: Basic Concepts and High Tech Bonding*, p 511. Elsevier, Amsterdam (2005)
31. Mark, J.E.: *Polymer Data Handbook*. 1018 (1999)
32. Mark, J.E., *Physical Properties of Polymers Handbook*. Springer Science and Business Media, New York (2007)
33. Rabinowicz, E., *Friction and Wear of Materials*, p 307. Wiley, New York (1995)
34. Khare, H.S., et al.: The interrelated effects of temperature and environment on wear and tribochemistry of an ultra-low wear PTFE composite. *J. Phys. Chem. C* (2015). doi:[10.1021/acs.jpcc.5b00947](https://doi.org/10.1021/acs.jpcc.5b00947)
35. Onodera, T., et al.: Effect of tribochemical reaction on transfer-film formation by poly(tetrafluoroethylene). *J. Phys. Chem. C* **118**, 11820–11826 (2014)
36. Tian, J., Xue, Q.J.: Surface modification of PTFE by Co-60 gamma-ray irradiation. *J. Appl. Polym. Sci.* **69**, 435–441 (1998)
37. Gong, D., Xue, Q.J., Wang, H.L.: Physical models of adhesive wear of polytetrafluoroethylene and its composites. *Wear* **147**, 9–24 (1991)
38. Hu, J.J., et al.: Transmission electron microscopy analysis of Mo-W-S-Se film sliding contact obtained by using focused ion beam microscope and in situ microtribometer. *Tribol. Lett.* **32**, 49–57 (2008)
39. Khare, H.S., Burris, D.L.: Surface and subsurface contributions of oxidation and moisture to room temperature friction of molybdenum disulfide. *Tribol. Lett.* **53**, 329–336 (2014)
40. Khare, H.S., Burris, D.L.: The effects of environmental water and oxygen on the temperature-dependent friction of sputtered molybdenum disulfide. *Tribol. Lett.* **52**, 485–493 (2013)